inhibitor of glucosaminyl-1-phosphate transferase, on the amounts and molecular weights of CaR in the absence or presence of MG132. Treatment with tunicamycin induced the appearance of unglycosylated CaR, with molecular weight of 115 kD (Figure 7A). Two differentially glycosylated forms of CaR were also observed, i.e., bands at molecular weights of 130 kD and 150 kD (Figure 7A), respectively. Previous studies have shown that the 130 kD form of CaR is the ER-localized high mannose-modified receptor, and the 150 kD CaR is the mature receptor at the plasma membrane (6,7). Addition of MG132 dramatically increased the amount of the 115 kD form of CaR (185.3 ± 29.6 % normalized to the amount in the absence of MG132), while the two glycosylated forms of CaR were increased to a lesser extent (130 kD form, 159.2 ± 12.6%; 150 kD form, 131 ± 10.3%) (Figure 7B). All forms of CaR are therefore sensitive to ubiquitination and degradation, although the immature forms of CaR (115 kD) which localize to the ER represent the strongest ubiquitination targets.

To determine whether dorfin-mediated ubiquitination is responsible for proteasomal degradation of the variously processed forms of CaR observed in the presence of tunicamycin, we cotransfected HEK293 cells with Flag-CaR with or without the dorfin dominant negative fragment, DCT, treated cells overnight with tunicamycin, and quantified the abundance of CaR forms on western blots (Figure 7C). As illustrated in the blot and associated graph (average of 3 independent experiments), the presence of DCT had an effect on CaR abundance comparable to addition of MG132 (compare Figure 7B and 7C), suggesting that ubiquitination leading to proteasomal degradation of all forms of CaR is mediated by dorfin.

To determine whether endogenous CaR is subjected to proteasome-dependent degradation in the ER, we tested whether MG132 could alter CaR protein levels in MDCK cells, which express endogenous CaR (24, 25) and endogenous dorfin (data not shown). MG132 significantly increased the tunicamycin-induced immature 115-kD form of CaR in MDCK cells (Figure 7D), suggesting that endogenous CaR is regulated by ERAD, presumably via a dorfin-mediated pathway.

DISCUSSION

The molecular mechanisms underlying the trafficking, targeting and turnover of CaR remain largely unknown. In this study we demonstrate that the E3 ubiquitin ligase dorfin, identified as a binding partner to the intracellular carboxyl terminus of CaR by Y2H screening of a human kidney library, interacts with CaR in HEK293 cells and regulates CaR abundance.

Dorfin contains two RING-finger domains and an In-between RING-finger domain at its amino terminus, through which it interacts specifically with the ubiquitin-conjugating enzymes Ubc7 and Ubc8 (11). In common with other RING domain E3 ubiquitin ligases, the dorfin carboxyl terminus confers specificity for substrate proteins including mutant superoxide dismutase-1 (12) and synphilin-1 (13). The region identified in the initial Y2H screen for CaR carboxyl

terminal binding partners corresponds to the distal carboxyl terminus of dorfin, from residues 561 to 838, further narrowed by directed Y2H screens to residues 660 to 838, implicating the distal carboxyl terminus of dorfin in binding to a range of its target proteins. Dorfin also interacts with VCP through its carboxyl terminus (14). It remains to be determined whether specific interaction motifs can be identified within the dorfin carboxyl terminus, which may aid in identifying additional dorfin targets.

Dorfin has been suggested to have role in the pathology of a variety of neurodegenerative diseases. Dorfin localizes to Lewy bodies in Parkinson's disease and dementia (12,14,26), and in Lewy body-like inclusions in amyotrophic lateral sclerosis (13,14). CaR is expressed in tissues that contribute to maintenance of systemic Ca^{2+} homeostasis, including the parathyroids, kidney, intestine and bones (1), as well as other cell types where its role(s) are less well-defined (27). Our results therefore suggest that dorfin may have more general roles as an E3 ligase in a variety of cells and tissues. Our data support a model in which dorfin mediates ubiquitination and proteasomal degradation of CaR via the ERAD pathway, which suggests that dorfin plays a crucial role in regulating the post-translational level of CaR. It will be of interest to determine whether alterations in CaR protein levels in CaR-related diseases are mediated by dorfin, given that endogenous CaR in MDCK cells is subject to ERAD.

The interactions between CaR and dorfin led us to investigate CaR ubiquitination. Ubiquitinated CaR is not observed in the absence of MG132, suggesting that ubiquitinated CaR is rapidly deubiquitinated or degraded. MG132 increased the overall amount of CaR protein, an effect mimicked by a dominant negative fragment of dorfin, suggesting that dorfin-mediated ubiquitination and proteasomal degradation play a significant role in regulating CaR protein. Ubiquitinated CaR immunoreactivity is observed over a wide range of molecular weights, 150 kD to more than 250 kD, typical of polyubiquitination, a potent signal for degradation (28,29). In addition, single point mutations of intracellular lysine residues to arginine did not significantly reduce CaR ubiquitination, suggesting that CaR is ubiquitinated at multiple lysine residues. Overall, our results demonstrate that CaR is multi/polyubiquitinated, and a target for proteasomal degradation.

Ubiquitination plays multiple roles in GPCR signaling. GPCR ubiquitination can occur in an agonist-induced manner or during receptor biosynthesis. Agonist-induced ubiquitination has been observed for yeast α-factor receptors (30,31), β2-adrenergic (32), chemokine CXCR4 (33), and vasopressin V2 receptors (34). Agonist-induced ubiquitination of GPCRs may regulate endosomal targeting, trafficking to lysosomes after endocytosis, or targeting to proteasomes for degradation (30-34). In addition to GPCRs, proteins which directly associate with GPCRs also undergo agonist-induced ubiquitination, including β-arrestins (32,35) and GRK2 (G protein-coupled receptor kinase 2) (36).

Agonist-independent ubiquitination has been observed for δ–opioid receptors

(37,38), rhodopsin (39,40), TRH receptors (41), and as described in the current report, CaR. Agonist-independent ubiquitination results from ERAD, i.e. misfolded, unfolded or abnormal proteins from the ER are retrotranslocated into the cytoplasm, deglycosylated and degraded by the proteasome (42). VCP is an AAA-ATPase that plays crucial roles in multiple aspects of the ERAD pathway in conjunction with its cofactors, Ufd1 and Ndl4 (16-19,42). Studies indicate that retrotranslocation of ERAD substrates from the ER and delivery to the proteasome is catalyzed by the VCP-Ufd1-Ndl4 complex, which binds first to polypeptide backbone and then the polyubiquitin chains on ERAD substrates. ATP hydrolysis catalyzed by VCP is required to complete retrotranslocation; VCP also chaperones polyubiquitinated proteins to the proteasome for degradation (42). Dorfin interacts with VCP, and has been colocalized with VCP in perinuclear aggresomes, i.e., membrane-free, cytoplasmic inclusions containing misfolded, ubiquitinated proteins (14), strongly suggesting the involvement of dorfin in the ERAD pathway. Immunoprecipitation of VCP with both CaR and dorfin from HEK293 cells supports the notion that CaR and dorfin interact at the ER. ERAD-mediated degradation of CaR is further supported by the observation that the tunicamycin-stabilized, unglycosylated form of CaR is most sensitive to MG132 treatment. The ability of the dominant negative fragment DCT to increase the abundance of all CaR forms demonstrates that proteasomal degradation of CaR is initiated by dorfin-mediated ubiquitination.

CaR is a disulfide linked dimer (1,5,8-10). CaR monomers have a large extracellular domain (ECD) of more than 600 amino acids (1). The ECD harbors 11 potential N-linked glycosylation sites, 8 of which are utilized (1,7). The CaR ECD also contains 19 cysteine residues; mutations at any of 14 cysteine residues abolish or dramatically reduce cell surface expression and/or function (1,9). N-linked glycosylation and disulfide bond formation occurs at the ER during membrane protein biosynthesis (43). Given the complexity of the structure of CaR, it is likely that some fraction of newly synthesized receptors are retained intracellularly for quality control purposes, as has been observed for both wt and mutant forms of CaR by western blotting (5-10); only properly glycosylated, dimerized and folded CaR are transported to Golgi complex and the plasma membrane (5-10). Dorfin may represent a critical step in the quality control mechanism, ensuring that only properly folded CaR exits the ER.

In summary, dorfin regulates ubiquitination and degradation of CaR via a VCP-mediated ERAD pathway. The molecular mechanisms underlying differential sorting of CaR to either the Golgi complex or the ERAD pathway remain to be explored.

ACKNOWLEDGEMENTS

We thank Dr. Klaus Seuwen (Novartis Pharma, AG) for human CaR, Dr. Richard Wojcikiewicz (SUNY Upstate Medical University) for HA-ubiquitin, and the members of the Breitwieser laboratory for helpful discussions. Supported by NIH GM 58578 and funds from the Weis Center for Research (GEB), and the graduate program of the Department of Biology, Syracuse University (YH).

REFERENCES

1. Brown, E.M., and Macleod, R.J. (2001) *Physiol. Rev.* **81**, 239-297
2. Brown, E.M., Gamba, G., Riccardi, D., Lombardi, M., Butters, R., Kifor, O., Sun, A., Hediger, M.A., Lytton, J., and Hebert, S.C. (1993) *Nature* **366**, 575-580
3. Romano, C., Yang, W., and O'Malley K.L. (1996) *J. Biol. Chem.* **271**, 28612-28616
4. White, J.H., Wise, A., Main, M.J., Green, A., Fraser, N.J., Disney, G.H., Barnes, A.A., Emson, P., Foord, S.M., and Marshall, F.H. (1998) *Nature* **386**, 679-6630
5. Bai, M., Trivedi, S., and Brown, E.M. (1998) *J. Biol. Chem.* **273**, 23605-23610
6. Fan, G., Goldsmith, P.K., Collins, R., Dunn, C.K., Krapcho, K.J., Rogers, K.V., and Spiegel, A.M. (1997) *Endocrinology* **138**, 1916-1922
7. Ray, K., Clapp, P., Goldsmith, P.K., and Spiegel, A.M. (1998) *J. Biol. Chem.* **273**, 34558-34567
8. Pace, A.J., Gama L., and Breitwieser G.E. (1999) *J. Biol. Chem.* **274**, 11629-11634
9. Ray, K., Hauschild, B.C., Steinbash, P.J., Goldsmith, P.K., Hauache, O., and Spiegel, A.M. (1999) *J. Biol. Chem.* **274**, 27642-27650
10. Bai, M., Trivedi S., Kifor, O., Quinn S.J., and Brown E.M. (1999) *Proc. Natl, Acad. Sci. U.S.A* **6**, 2834-2839
11. Niwa, J., Ishigaki, S., Doyu, M., Suzuki, T., Tanaka, K., and Sobue, G. (2001) *Biochem. Biophys. Res. Commun.* **281**, 706-713
12. Niwa, J., Ishigaki, S., Hishikawa, N., Yamamoto, M., Doyu, M., Murata, S., Tanaka, K., Taniguchi, N., and Sobue, G. (2002) *J. Biol. Chem.* **277**, 36793-36798
13. Ito, T., Niwa, J., Hishikawa, N., Ishigaki, S., Doyu, M., and Sobue, G. (2003) *J. Biol. Chem.* **278**, 29106-29114
14. Ishigaki, S., Hishikawa, N., Niwa, J., Iemura, S., Natsume, T., Hori, S., Kakizuka, A., Tanaka, K., and Sobue, G. (2004) *J. Biol. Chem.* **279**, 51376-51385
15. Wojcikiewicz, R.J.H. (2004) *Trends. Pharmacol. Sci.* **25**, 35-41
16. Ye, Y., Meyer, H.H., and Rapoport, T.A. (2001) *Nature* **6864**, 652-656
17. Dai, R.M., and Li, C.C. (2001) *Nat. Cell. Biol.* **8**, 740-744
18. Jarosch, E., Taxis, C., Volkwein, C., Bordallo, J., Finley, D., Wolf, D.H., and Sommer, T. (2002) *Nat. Cell. Biol.* **4**, 134-139
19. Robinovich, E., Kerem, A., Frohlich, K.U., Diamant, N., and Bar-Nun, S. (2002) *Mol. Cell.Biol.* **22** 626-634
20. Goldsmith, P.K., Fan, G., Miller, J.L., Rogers, K.V., and Spiegel, A.M. (1997) *J. Bone. Miner. Res.* **12**, 1780-1788
21. Zhang, M., and Breitwieser, G.E. (2005) *J. Biol. Chem.* **280**, 11140-11146
22. Gama, L., and Breitwieser, G.E. (1999) *BioTechniques* **26**, 814-815

23. Gietz, R.D., and Schiestl, R.H. (1995) *Methods Mol. Cell. Biol.* **5**, 255-269
24. Arthur, J.M., Collinsworth, G.P., Gettys, T.W., Quarles, L.D., and Raymond, J.R. (1997) *Am. J. Physiol. Renal. Physiol.* **273**, F129-F135
25. Arthur, J.M., Lawrence, M.S., Payne, C.R., Rane, M.J., and McLeish, K.R. (2000) *Biochem. Biophys. Res. Commun.* **275**, 538-541
26. Hishikawa, N., Niwa, J., Doyu, M., Ito, T., Ishigaki, S., Hashizume, Y., and Sobue, G. (2003) *Am. J. Pathol.* **163**, 609-619
27. Peace, S.H.S., and Thakker, R.V. (1997) *J. Endocrinol.* **154**, 371-378
28. Pickart, C.M. (2001) *Annu. Rev. Biochem.* **70**, 503-533
29. Weissman, A.M. (2001) *Nat. Rev. Mol. Cell Biol.* **2**, 169-178
30. Roth, A.F., and Davis, N.G. (1996) *J.Cell Biol.* **134**,661-674
31. Hicke, L. and Riezman, H. (1996) *Cell* **84**, 277-287
32. Shenoy, S.K., McDonald, P.H., Kohout, T.A., and Lefkowitz, R.J. (2001) *Science* **294**, 1307-1313
33. Marchese, A., and Benovic, J.L. (2001) *J. Biol. Chem.* **276**,45509-45512
34. Martin, N.P., Lefkowitz, R.J., and Shenoy, S.K. (2003) *J. Biol. Chem.* **278**, 45954-45959
35. Shenoy, S.K., and Lefkowitz, R.J. (2003) *J. Biol. Chem.* **278**, 14498-14506
36. Penela, P., Ruiz-Gomez, A., Castano, J.G., and Mayor, F.J. (1998) *J. Biol. Chem.* **273**, 35238-35244
37. Petaja-Repo, U.E., Hogue, M., Laperriere, A., Bhalla, S., Walker, P., and Bouvier, M. (2001) *J. Biol. Chem.* **276**, 4416-4423
38. Chaturvedi, K., Bandari, P., Chinen, N., and Howells, R.D. (2001) *J. Biol. Chem.* **276**, 12345-12355
39. Saliba, R.S., Munro, P.M.G., Luthert, P.J., and Cheetham, M.E. (2002) *J. Cell Sci.* **115**, 2907-2918
40. Illing, M.E., Rajan, R.S., Bence, N.F., and Kopito, R.R. (2002) *J. Biol. Chem.* **37**, 34150-34160
41. Cook, L.B., Zhu, C.C., and Hinkle, P.M. (2003) *Mol. Endocrinol.* **17**, 1777-1791
42. Meusser, B., Hirsch, C., Jarosch, E., and Sommer, T. (2005) *Nat. Cell. Biol.* **7**, 766-772
43. Kostova, Z., and Wolf, D.H. (2003) *EMBO Journal* **22**, 2309-2317

ABBREVIATIONS

The abbreviations used are: CaR, calcium sensing receptor; CT, carboxyl terminus; DCT, dorfin carboxyl terminal dominant negative fragment; ER, endoplasmic reticulum; ERAD, endoplasmic reticulum-associated degradation; GPCR, G protein-coupled receptor; VCP, valosin-containing protein; HEK293, human embryonic kidney 293; MDCK, Madin-Darby canine kidney; EGFP, enhanced green fluorescence protein; PBS, phosphate-buffered saline; RING, really interesting new gene; Y2H assay, yeast two-hybrid assay

FIGURE LEGENDS

Figure 1. Analysis of interaction sites on calcium-sensing receptor (CaR) and the E3 ubiquitin ligase dorfin by directed Y2H assay. (A). Schematic representation of CaR and localization of the interaction site for dorfin carboxyl terminal fragment (residues 561-838). The cytoplasmic carboxyl terminus of CaR (residues 866 to 1078) was truncated from both the amino and carboxyl termini as indicated, and screened by cotransformation of the AH109 yeast strain with the CaR fragment plus the carboxyl terminal of dorfin (residues 561-838). TM, transmembrane heptahelical domain; ECD, extracellular domain. (B). Schematic representation of dorfin and localization of the interaction site for CaR carboxyl terminal fragment (residues 866-1078). Truncations were generated from both the amino and carboxyl terminal ends of the dorfin fragment (residues 561-838) and screened by cotransformation of the AH109 yeast strain with the dorfin fragment plus the carboxyl terminus of CaR (residues 866-1078). R1, R2, RING finger domains; IBR, in between RING-finger domain. For (A) and (B), positive interactions, resulting in activation of three reporter genes (HIS3, ADE2 and MEL1) are indicated as +.

Figure 2. Interaction of full length CaR and dorfin in HEK293 cells. (A). HEK293 cells were transfected with (lane 1) or without (lane 2) Flag-CaR cDNA. Cells were harvested 72 hours after transfection. Anti-Flag antibody was used to immunoprecipitate samples, and blots were probed with anti-dorfin antibody D-30 (top panel). Lysates were probed with anti-dorfin D-30 antibody (middle panel) or anti-CaR LRG antibody (bottom panel) to assess protein expression. (B). Flag-CaR cDNA transfected HEK293 cells were cotransfected with EGFP-dorfin (lane 1), DNT-EGFP (lane 2) or DCT-EGFP (lane 3), respectively. Anti-Flag antibody was used to immunoprecipitate samples, and blots were probed with anti-GFP antibody (top panel). Lysates were probed with anti-GFP antibody (middle panel) or anti-CaR LRG antibody (lower panel) to assess protein expression.

Figure 3. Ubiquitination of CaR in HEK293 cells. (A). Flag-CaR or Flag-CaR(0K) cDNA was transfected into HEK293 cells with HA-Ub cDNA. Cells were incubated without (lanes 1, 3) or with (lanes 2, 4) 10 μM proteasomal inhibitor MG132 for 12 hrs prior to lysis. Cell lysates were immunoprecipitated with anti-Flag antibody and the precipitated pellets were treated with 1% SDS/PBS to disrupt non-covalent interactions. Supernatants were diluted with lysis buffer, followed by a second immunoprecipitation using anti-Flag antibody. The blot was probed with anti-HA antibody (upper panel). The same blot was then stripped and probed with anti-CaR antibody LRG (lower panel). (B). Flag-CaR cDNA or Flag-CaR(0K) cDNA was transfected into HEK293 cells. Cells were preincubated with 0.5 mM Ca^{2+} overnight prior to exposure to either 0.5 or 5 mM Ca^{2+} for 10 min (37°C), followed by immunoblotting of lysates with anti-phospho-ERK1/2 antibody. (C). Flag-CaR cDNA or Flag-CaR(0K) cDNA was transfected into HEK293 cells. Anti-Flag antibody was used to immunoprecipitate samples, and blots were probed with anti-dorfin D-30 antibody (top blot). Lysates were probed with anti-dorfin D-30 antibody (middle blot) or anti-CaR LRG antibody (bottom blot).

Figure 4. Regulation of CaR ubiquitination by dorfin. (A). Dorfin mediates ubiquitination of CaR. Flag-CaR (3 μg) and HA-Ub (2 μg) cDNAs were cotransfected into HEK293 cells, without (-) or with (+) EGFP-dorfin cDNA (6 μg). Cells were incubated with 10 μM MG132 for 12 hrs prior to lysis. Cell lysates were immunoprecipitated with anti-Flag antibody and blots probed with anti-HA antibody. CaR ubiquitination was quantified and normalized to basal ubiquitination in the absence of exogenous dorfin; significance at * $p < 0.05$. (B). Dominant negative dorfin fragment DCT inhibits ubiquitination of CaR. Flag-CaR cDNA (3 μg) and HA-ubiquitin cDNA (2 μg) were cotransfected into HEK293 cells, without (-) or with (+) DCT-EGFP cDNA (6 μg). Methods as described in (A).

Figure 5. Regulation of steady-state protein level of CaR by dorfin. (A). Wild-type dorfin enhances degradation of CaR. Flag-CaR cDNA (1 μg) was transfected into HEK293 cells with increasing amounts of EGFP-dorfin cDNA (0, 2, 4, or 6 μg). Cell lysates were probed for Flag-CaR, endogenous actin and EGFP-dorfin by immunoblotting with anti-CaR (LRG), anti-actin, or anti-GFP antibodies. Graph (average of 3 independent experiments) indicates normalized CaR protein or EGFP-dorfin as a function of transfected EGFP-dorfin cDNA. CaR protein was normalized to amount in the absence of exogenous EGFP-dorfin; EGFP-dorfin normalized to that observed at 6 μg EGFP-dorfin cDNA. Filled circles, Flag-CaR; open circles, EGFP-dorfin. (B). Dominant negative construct of dorfin (DCT-EGFP) stabilizes CaR. Flag-CaR cDNA (1 μg) was transfected into HEK293 cells with increasing amounts of DCT-EGFP cDNA (0, 2, 4, or 6 μg). The remaining procedures were described in (A). Graph (average of 3 independent experiments) indicates normalized CaR protein or DCT-EGFP, normalized as described in (A). Filled circles, Flag-CaR; open circles, DCT-EGFP. For both (A), (B), significance at * $p < 0.05$. (C). Flag-CaR cDNA (1 μg) was transfected into HEK293 cells without (lane 1) or with EGFP-dorfin (6 μg) (lanes 2 and 3). Cells were treated without (lanes 1 and 2) or with (lane 3) MG132 for 12 hours before lysis. Cell lysates were probed for Flag-CaR by immunoblotting with anti-CaR LRG antibody.

Figure 6. VCP/CaR/Dorfin coimmunoprecipitation in HEK293 cells. HEK293 cells were transfected without (-) or with (+) Flag-CaR cDNA. Cell lysates were immunoprecipitated with anti-VCP antibody and western blots probed with anti-CaR antibody LRG (first blot). The same blot was stripped and reprobed with anti-dorfin antibody D-30 (second blot). The expression of endogenous VCP, transfected CaR, and endogenous dorfin were confirmed by immunoblotting cell lysates with anti-VCP antibody (third blot), anti-CaR LRG antibody (fourth blot), or anti-dorfin D-30 antibody (fifth blot).

Figure 7. Sensitivity of immature forms of CaR to proteasomal degradation. (A). Tunicamycin stabilizes an immature form of CaR. HEK293 cells transfected with Flag-CaR cDNA were treated without or with tunicamycin (5 μg/ml) for twelve hours prior to lysis. Lysates were immunoprecipitated with anti-Flag antibody and probed with anti-CaR LRG antibody. (B). MG132 increases the amounts of immature forms of CaR. HEK293 cells were transfected with Flag-CaR and HA-Ub cDNAs, and incubated with tunicamycin (5 μg/ml) without or with MG132 (10 μM), for 12 hrs prior to lysis. Lysates were immunoprecipitated with anti-Flag antibody and probed with anti-CaR LRG antibody. Three forms of CaR are

evident in tunicamycin, 1, fully glycosylated CaR (150 kD); 2, ER-resident high-mannose CaR (130 kD); 3, unglycosylated CaR (115 kD). The amount of CaR protein in each form was quantified in the absence or presence of MG132, and average results for 3 independent experiments are illustrated (each band normalized to the amount observed in the absence of MG132), significance at * $p < 0.05$. (C). DCT increases the amounts of immature forms of CaR. HEK293 cells were transfected with Flag-CaR without or with DCT-EGFP. Cells were incubated with tunicamycin (5 mg/ml) for 12 hrs prior to lysis. Experiments as in (A). Graph indicates amounts of 3 forms of CaR protein in the absence or presence of DCT-EGFP, normalized to the amount in the absence of DCT-EGFP. Significance at * $p < 0.05$. (D). MG132 increases the amounts of immature CaR in MDCK cells. MDCK cells were treated with tunicamycin (5 μg/ml) without or with MG132 (10 μM) for 12 hrs prior to lysis. Lysates were immunoblotted with anti-CaR LRG antibody.

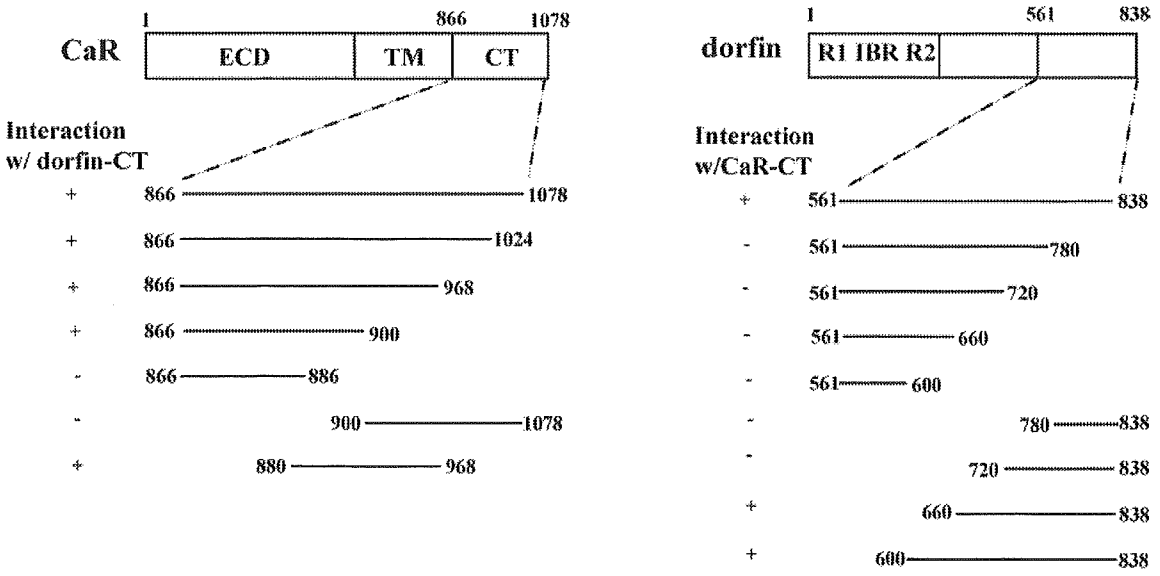
A.
CaR
1
866
1078
ECD
TM
CT
Interaction
w/ dorfin-CT
+ 866 1078
+ 866 1024
+ 866 968
+ 866 900
- 866 886
- 900 1078
+ 880 968
B.
dorfin
1
561
838
R1 IBR R2
Interaction
w/CaR-CT
+ 561 838
- 561 780
- 561 720
- 561 660
- 561 600
- 780 838
- 720 838
+ 660 838
+ 600 838

Figure 1

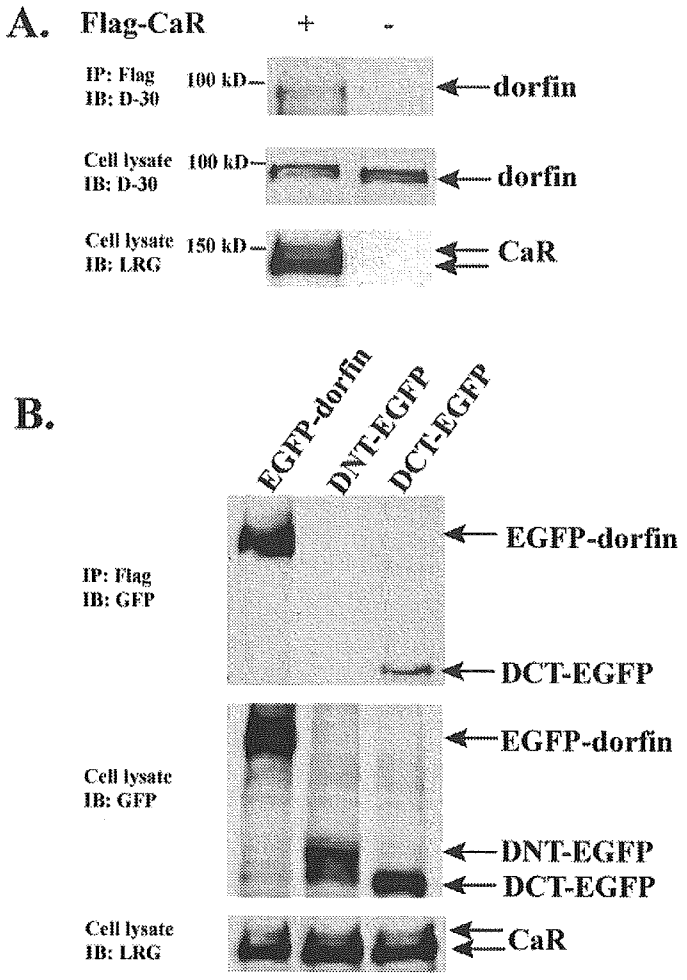
A.
Flag-CaR
+
-
IP: Flag
IB: D-30
100 kD
dorfin
Cell lysate
IB: D-30
100 kD
dorfin
Cell lysate
IB: LRG
150 kD
CaR
B.
EGFP-dorfin
DNT-EGFP
DCT-EGFP
IP: Flag
IB: GFP
EGFP-dorfin
DCT-EGFP
Cell lysate
IB: GFP
EGFP-dorfin
DNT-EGFP
DCT-EGFP
Cell lysate
IB: LRG
CaR

Figure 2

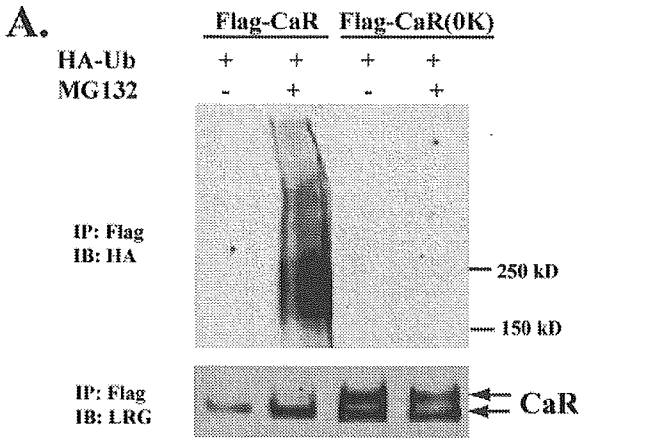
A.
Flag-CaR
Flag-CaR(0K)
HA-Ub
+ + + +
MG132
- + - +
IP: Flag
IB: HA
250 kD
150 kD
IP: Flag
IB: LRG
CaR

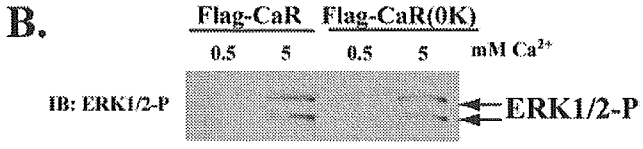
B.
Flag-CaR
Flag-CaR(0K)
0.5 5 0.5 5 mM Ca2+
IB: ERK1/2-P
ERK1/2-P

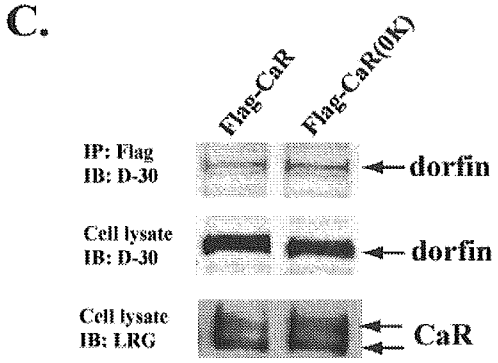
C.
Flag-CaR
Flag-CaR(0K)
IP: Flag
IB: D-30
dorfin
Cell lysate
IB: D-30
dorfin
Cell lysate
IB: LRG
CaR

Figure 3

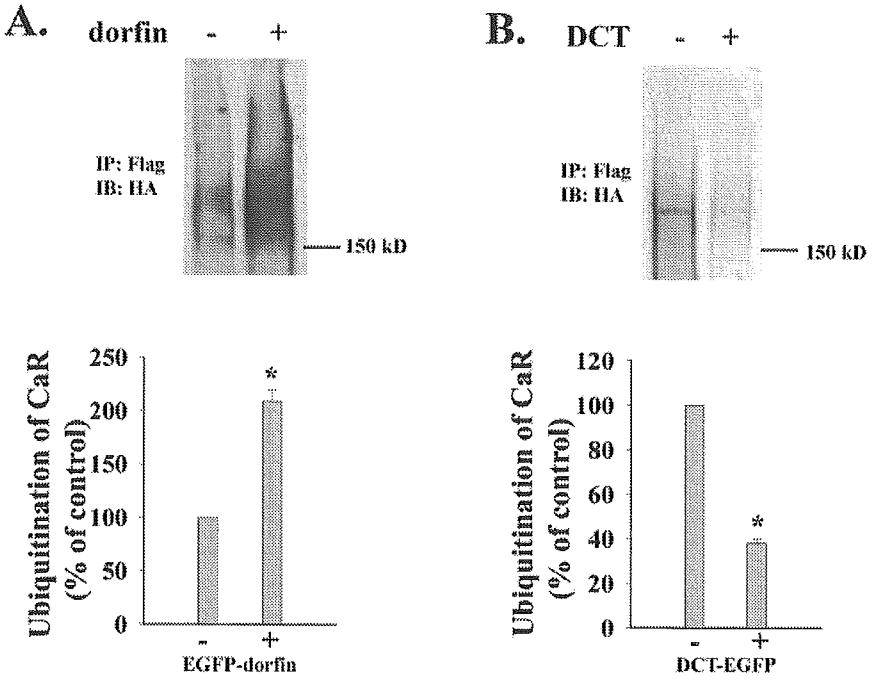
A.
dorfin
-
+
IP: Flag
IB: HA
150 kD
Ubiquitination of CaR
(% of control)
250
200
150
100
50
0
*
-
+
EGFP-dorfin
B.
DCT
-
+
IP: Flag
IB: HA
150 kD
Ubiquitination of CaR
(% of control)
120
100
80
60
40
20
0
*
-
+
DCT-EGFP

Figure 4

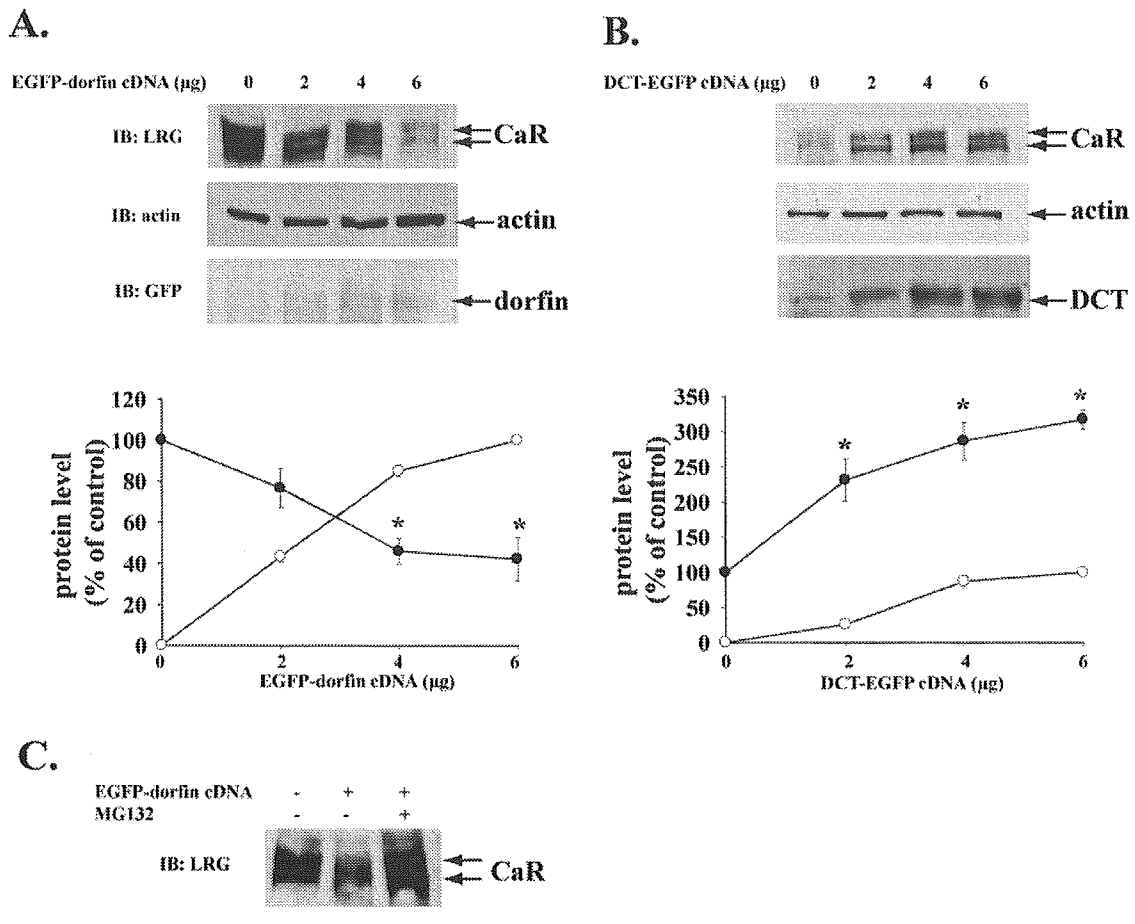
A.
EGFP-dorfin cDNA (μg) 0 2 4 6
IB: LRG
CaR
IB: actin
actin
IB: GFP
dorfin
protein level (% of control)
EGFP-dorfin cDNA (μg)
B.
DCT-EGFP cDNA (μg) 0 2 4 6
CaR
actin
DCT
protein level (% of control)
DCT-EGFP cDNA (μg)
C.
EGFP-dorfin cDNA - + +
MG132 - - +
IB: LRG
CaR

Figure 5

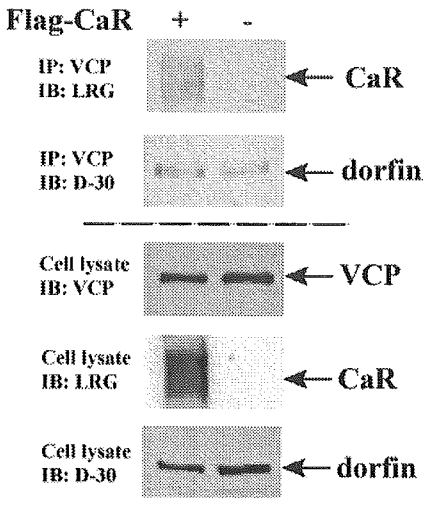
Flag-CaR + -
IP: VCP
IB: LRG
CaR
IP: VCP
IB: D-30
dorfin
Cell lysate
IB: VCP
VCP
Cell lysate
IB: LRG
CaR
Cell lysate
IB: D-30
dorfin

Figure 6

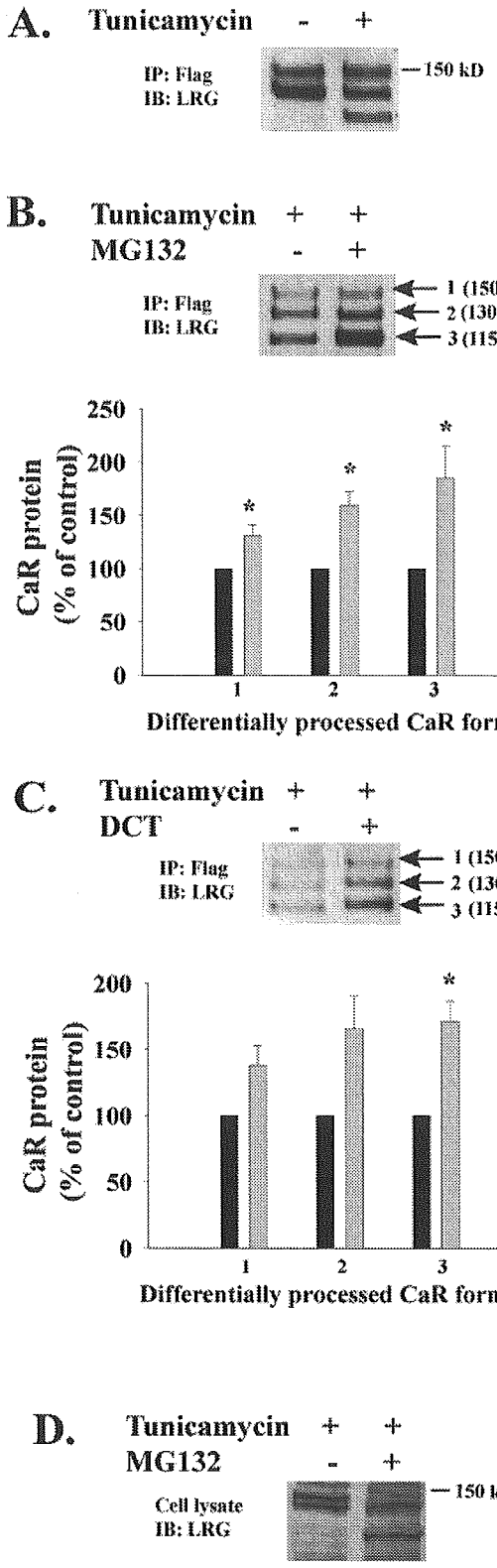
A.
Tunicamycin - +
IP: Flag
IB: LRG
150 kD
B.
Tunicamycin + +
MG132 - +
IP: Flag
IB: LRG
1 (150 kD)
2 (130 kD)
3 (115 kD)
CaR protein (% of control)
250
200
150
100
50
0
1
2
3
Differentially processed CaR forms
C.
Tunicamycin + +
DCT - +
IP: Flag
IB: LRG
1 (150 kD)
2 (130 kD)
3 (115 kD)
CaR protein (% of control)
200
150
100
50
0
1
2
3
Differentially processed CaR forms
D.
Tunicamycin + +
MG132 - +
Cell lysate
IB: LRG
150 kD

Figure 7

YEXNR-09109; No. of pages: 11; 4C: 3, 6, 8, 9

Available online at www.sciencedirect.com

SCIENCE DIRECT®

Experimental Neurology xx (2006) xxx–xxx

Experimental Neurology

www.elsevier.com/locate/yexnr

Review

Pathogenesis, animal models and therapeutics in Spinal and bulbar muscular atrophy (SBMA)

Masahisa Katsuno, Hiroaki Adachi, Masahiro Waza, Haruhiko Banno, Keisuke Suzuki, Fumiaki Tanaka, Manabu Doyu, Gen Sobue *

Department of Neurology, Nagoya University Graduate School of Medicine, 65 Tsurumai-cho, Showa-ku, Nagoya 466-8550, Japan

Received 12 December 2005; revised 18 January 2006; accepted 20 January 2006

Abstract

Spinal and bulbar muscular atrophy (SBMA) is a hereditary neurodegenerative disease characterized by slowly progressive muscle weakness and atrophy of bulbar, facial, and limb muscles. The cause of SBMA is expansion of a trinucleotide CAG repeat, which encodes the polyglutamine tract, in the first exon of the androgen receptor (AR) gene. SBMA chiefly occurs in adult males, whereas neurological symptoms are rarely detected in females having mutant AR gene. The cardinal histopathological finding of SBMA is loss of lower motor neurons in the anterior horn of spinal cord as well as in brainstem motor nuclei. Animal models carrying human mutant AR gene recapitulate polyglutamine-mediated motor neuron degeneration, providing clues to the pathogenesis of SBMA. There is increasing evidence that testosterone, the ligand of AR, plays a pivotal role in the pathogenesis of neurodegeneration in SBMA. The striking success of androgen deprivation therapy in SBMA mouse models has been translated into clinical trials. In addition, elucidation of pathophysiology using animal models leads to emergence of candidate drugs to treat this devastating disease: HSP inducer, Hsp90 inhibitor, and histone deacetylase inhibitor. Utilizing biomarkers such as scrotal skin biopsy would improve efficacy of clinical trials to verify the results from animal studies. Advances in basic and clinical researches on SBMA are now paving the way for clinical application of potential therapeutics.

Keywords: Spinal and bulbar muscular atrophy; Polyglutamine; Androgen receptor; Testosterone; Luteinizing hormone-releasing hormone analog; Heat shock protein; Geranylgeranylacetone; 17-Allylamino geldanamycin; Histone deacetylase inhibitor; Axonal transport

Contents

History and nomenclature . . . 0
Clinical features . . . 0
Etiology . . . 0
Pathology . . . 0
Molecular pathogenesis and therapeutic strategies . . . 0
Ligand-dependent pathogenesis in animal models of SBMA . . . 0
Testosterone blockade therapy for SBMA . . . 0
Role of heat shock proteins in pathogenesis of SBMA . . . 0
Transcriptional dysregulation in SBMA . . . 0
Axonal trafficking defects in SBMA . . . 0
Clinical application of potential therapeutics . . . 0
Acknowledgments . . . 0
References . . . 0

* Corresponding author. Fax: +81 52 744 2384.
E-mail address: sobueg@med.nagoya-u.ac.jp (G. Sobue).

0014-4886/$ - see front matter © 2006 Elsevier Inc. All rights reserved.
doi:10.1016/j.expneurol.2006.01.021

History and nomenclature

More than a hundred years have elapsed since the first description of spinal and bulbar muscular atrophy (SBMA) from Hiroshi Kawahara, who described the clinical and hereditary characteristics of two Japanese brothers with progressive bulbar palsy (Kawahara, 1897). This work was followed by several reports on similar cases with or without X-linked pattern of inheritance (Katsuno et al., 2004). SBMA is also known as Kennedy disease (KD), named after William R. Kennedy, whose study on 11 patients from 2 families depicted the clinical, genetical, and pathological features of this disorder (Kennedy et al., 1968). Other names for this disease are bulbospinal neuronopathy and bulbospinal muscular atrophy.

In 1991, the cause of SBMA was identified as the expansion of a trinucleotide CAG repeat in the androgen receptor (AR) gene (La Spada et al., 1991). This was the first discovery of polyglutamine-mediated neurodegenerative diseases, and subsequent studies using transgenic animal models opened the door to development of pathogenesis-based therapies for this devastating disease.

Clinical features

SBMA exclusively affects adult males. The prevalence of this disease is estimated to be 1–2 per 100,000, whereas a considerable number of patients may have been misdiagnosed as other neuromuscular diseases including amyotrophic lateral sclerosis (Fischbeck, 1997). Patients of various ethnic backgrounds have been reported around the world.

Major symptoms of SBMA are weakness, atrophy, and fasciculations of bulbar, facial and limb muscles (Sperfeld et al., 2002; Katsuno et al., 2004). In extremities, involvement is usually predominant in proximal musculature. The onset of weakness is usually between 30 and 60 years but is often preceded by nonspecific symptoms such as postural tremor and muscle cramps. Although fasciculations in the extremities are rarely present at rest, they are easily induced when patients hold their arms horizontally or bend their legs while lying on their backs. These contraction fasciculations are especially noticeable in the face, neck, and tongue and are usually present in the early stage. Fatigability after exercise might also be accompanied. Bilateral facial and masseter muscle weakness, poor uvula and soft palatal movements, and atrophy of the tongue with fasciculations are often encountered. Speech has a nasal quality in most cases due to reduced velopharyngeal closure. Advanced cases often develop dysphagia, eventually resulting in aspiration or choking. Muscle tone is usually hypotonic, and no pyramidal signs are detected. Deep tendon reflex is diminished or absent with no pathological reflex. Sensory involvement is largely restricted to vibration sense which is affected distally in the legs. Cerebellar symptoms, dysautonomia, and cognitive impairment are absent. Patients occasionally demonstrate signs of androgen insensitivity such as gynecomastia, testicular atrophy, dyserection, and decreased fertility, some of which are detected before the onset of motor symptoms. Abdominal obesity is common, whereas male pattern baldness is rare in patients with SBMA.

Electromyogram shows neurogenic abnormalities, and distal motor latencies are often prolonged in nerve conduction study. Both sensory nerve action potential and sensory evoked potential are reduced or absent. Endocrinological examinations frequently reveal partial androgen resistance with elevated serum testosterone level. Serum creatine kinase level is elevated in the majority of patients. Hyperlipidemia, liver dysfunction, and glucose intolerance are also detected in some patients. Profound facial fasciculations, bulbar signs, gynecomastia, and sensory disturbance are the main clinical features distinguishing SBMA from other motor neuron diseases, although gene analysis is indispensable for diagnosis. Female patients are usually asymptomatic, but some express subclinical phenotypes including high amplitude motor unit potentials on electromyography (Sobue et al., 1993).

The progression of SBMA is usually slow, but a considerable number of patients need assistance to walk in their fifties or sixties. Life-threatening respiratory tract infection often occurs in the advanced stage of the disease, resulting in early death in some patients. No specific therapy for SBMA has been established. Testosterone has been used in some patients, although it has no effects on the progression of SBMA.

Etiology

The cause of SBMA is expansion of a trinucleotide CAG repeat, which encodes the polyglutamine tract, in the first exon of the androgen receptor (AR) gene (La Spada et al., 1991). The CAG repeat within AR ranges in size from 9 to 36 in normal subjects but from 38 to 62 in SBMA patients. Expanded polyglutamine tracts have been found to cause several neurodegenerative diseases including SBMA, Huntington's disease, several forms of spinocerebellar ataxia, and dentatorubral-pallidoluysian atrophy (Gatchel and Zoghbi, 2005). These disorders, known as polyglutamine diseases, share salient clinical features including anticipation and somatic mosaicism, as well as selective neuronal and nonneuronal involvement despite widespread expression of the mutant gene. There is an inverse correlation between the CAG repeat size and the age at onset or the disease severity adjusted by the age at examination in SBMA as documented in other polyglutamine diseases (Doyu et al., 1992). These observations explicitly suggest that common mechanisms underlie the pathogenesis of polyglutamine diseases.

AR, the causative protein of SBMA, is an 110-kDa nuclear receptor which belongs to the steroid/thyroid hormone receptor family (Poletti, 2004). AR mediates the effects of androgens, testosterone, and dihydrotestosterone, through binding to an androgen response element in the target gene to regulate its expression. AR is essential for major androgen effects including normal male sexual differentiation and pubertal sexual development, although AR-independent nongenomic function of androgen has been reported. AR is expressed not only in primary and secondary sexual organs but also in nonreproductive organs including the kidney, skeletal muscle, adrenal gland, skin, and nervous system, suggesting its far-reaching influence on a variety of mammalian tissues. In the central nervous system, the expression level of AR is relatively high in spinal and brainstem

motor neurons, the same cells which are vulnerable in SBMA. The AR gene is located on chromosome Xq11–12. This 90-kb DNA contains eight exons coding for the functional domains specific to the nuclear receptor family. The first exon codes for the N-terminal transactivating domain. Exons 2 and 3 code for the DNA-binding domain, whereas exons 4 through 8 code for the ligand-binding domain. The N-terminal transactivating domain, in which a CAG trinucleotide repeat locates, possesses a major transactivation function maintained by interaction with general transcriptional coactivators such as c-AMP response element binding protein-binding protein (CBP), TAFII130, and steroid receptor coactivator-1 (SRC-1). The CAG repeat beginning at codon 58 in the first exon of AR encodes polyglutamine tract. The length of this repeat is highly variable because of the slippage of DNA polymerase upon DNA replication. Whereas its abnormal elongation causes SBMA, the shorter CAG repeat is likely to increase the risk of prostate cancer (Clark et al., 2003). Transcriptional coactivators also possess glutamine-rich regions modulating protein–protein interaction with the N-terminal transactivating domain of AR.

The expansion of a polyglutamine tract in AR has been implicated in the pathogenesis of SBMA in two different, but not mutually exclusive, ways: loss of normal AR function induces neuronal degeneration; and the pathogenic AR acquires toxic property damaging motor neurons. Since AR possesses trophic effects on neuronal cells, one can assume that loss of AR function may play a role in the pathogenesis of SBMA. Expansion of the polyglutamine tract mildly suppresses the transcriptional activities of AR, probably because it disrupts interaction between the N-terminal transactivating domain of AR and transcriptional coactivators (Poletti, 2004). Although this loss of function of AR may contribute to the androgen insensitivity in SBMA, the pivotal cause of neurodegeneration in SBMA has been believed to be a gain of toxic function of the pathogenic AR due to expansion of the polyglutamine tract. This hypothesis is supported by the observation that motor impairment has never been observed in severe testicular feminization (Tfm) patients lacking AR function or in AR knockout mice. Moreover, a transgenic mouse model carrying an elongated CAG repeat driven by human AR promoter demonstrated motor impairment, suggesting that the expanded polyglutamine tract is sufficient to induce the pathogenic process of SBMA (Adachi et al., 2001).

Aggregation of abnormal protein has been considered to be central to the pathogenesis of neurodegenerative diseases such as Alzheimer disease, Parkinson disease, amyotrophic lateral sclerosis, and prion disease. An expanded polyglutamine stretch alters conformation of causative proteins, resulting in aggregation of the proteins. It is now widely accepted that aggregation of these abnormal proteins in neurons is the primary event in the pathogenesis of polyglutamine diseases. The rate-limiting step of aggregation has been proposed to be the formation of oligomeric nucleus, which may occur form after a repeat length-dependent conformational change of polyglutamine monomer from a random coil to a parallel, helical β-sheet (Wyttenbach, 2004). Several experimental observations indicate that formation of toxic oligomers, or intermediates, of abnormal polyglutamine-containing protein instigates a series of cellular events which lead to neurodegeneration (Muchowski and Wacker, 2005). This hypothesis is likely to be the case in SBMA.

Pathology

Histopathological studies provide important information on the pathogenesis of polyglutamine-mediated neurodegeneration. The fundamental histopathological finding of SBMA is loss of lower motor neurons in the anterior horn of spinal cord as well as in brainstem motor nuclei except for the third, fourth and sixth cranial nerves (Fig. 1A) (Sobue et al., 1989). The

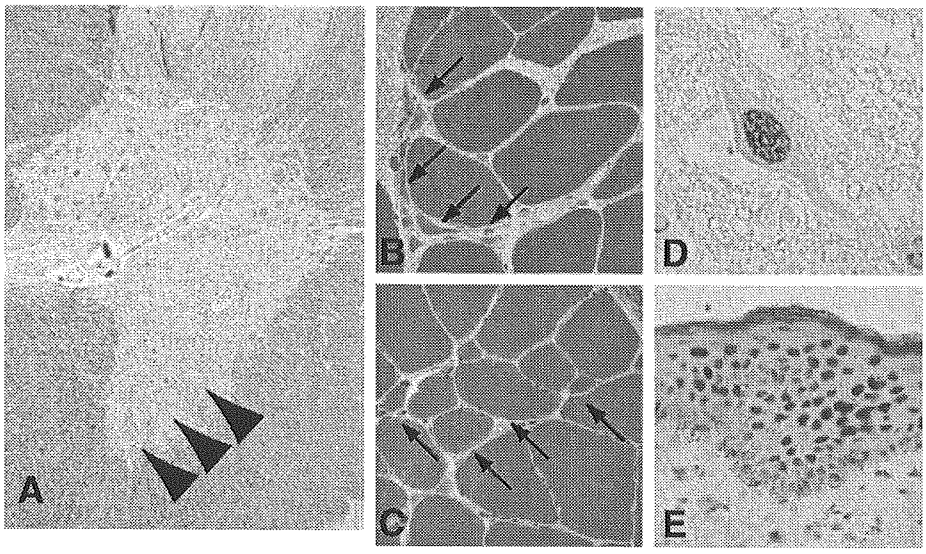

Fig. 1. Histopathology of SBMA. (A) A transverse section of spinal cord demonstrates marked depletion of motor neurons in the anterior horn. (B and C) HE staining of skeletal muscle shows both neurogenic (B, arrows) and myogenic changes (C, arrows). (D) A residual motor neuron in the lumbar anterior horn shows a diffuse nuclear accumulation of pathogenic androgen receptor detected by anti-polyglutamine antibody. (E) Nuclear accumulation of pathogenic AR is also detected in nonneuronal tissues such as scrotal skin (E).

number of nerve fibers is reduced in the ventral spinal nerve root, reflecting motor neuronopathy. Sensory neurons in the dorsal root ganglia were less severely affected, and large myelinated fibers demonstrate a distally accentuated sensory axonopathy in the peripheral nervous system. Neurons in the Onufrowicz nuclei, intermediolateral columns, and Clarke's columns of the spinal cord are generally well preserved. Muscle histopathology includes both neurogenic and myogenic findings: there are groups of atrophic fibers with a number of small angular fibers, fiber type grouping and clamps of pyknotic nuclei as well as variability in fiber size, hypertrophic fibers, scattered basophilic regenerating fibers, and central nuclei (Figs. 1B and C).

A pathologic hallmark of polyglutamine diseases is the presence of nuclear inclusions (NIs). In SBMA, NIs containing the pathogenic AR are found in the residual motor neurons in the brainstem and spinal cord as well as in nonneuronal tissues including prostate, testis, and skin (Li et al., 1998). These inclusions are detectable using antibodies recognizing a small portion of the N-terminus of the AR protein, but not by those against the C-terminus of the protein. This observation implies that the C-terminus of AR is truncated or masked upon formation of NI. A full-length AR protein with expanded polyglutamine tract is cleaved by caspase-3, liberating a polyglutamine-containing toxic fragment, and the susceptibility to cleavage is polyglutamine repeat length-dependent (Kobayashi et al., 1998). Thus, proteolytic cleavage is likely to enhance the toxicity of the pathogenic AR protein. Electron microscopic immunohistochemistry shows dense aggregates of AR-positive granular material without limiting membrane, both in the neural and nonneural inclusions, in contrast to the other polyglutamine diseases in which NIs take the form of filamentous structures. Although NI is a disease-specific histopathological finding, its role in pathogenesis has been heavily debated. Several studies have suggested that NI may indicate cellular response coping with the toxicity of abnormal polyglutamine protein (Arrasate et al., 2004). Instead, the diffuse nuclear accumulation of the mutant protein has been considered essential for inducing neurodegeneration in polyglutamine diseases including SBMA.

An immunohistochemical study on autopsied SBMA patients using an anti-polyglutamine antibody demonstrates that diffuse nuclear accumulation of the pathogenic AR is more frequently observed than NIs in the anterior horn of spinal cord (Adachi et al., 2005). Intriguingly, the frequency of diffuse nuclear accumulation of the pathogenic AR in spinal motor neurons strongly correlates with the length of the CAG repeat in the AR gene. No such correlation has been found between NI occurrence and the CAG repeat length. Similar findings have also been reported on other polyglutamine diseases. Taken together, it appears that the pathogenic AR containing an elongated polyglutamine tract principally accumulates within the nuclei of motor neurons in a diffusible form, leading to neuronal dysfunction and eventual cell death. In support of this hypothesis, neuronal dysfunction is halted by genetic modulation preventing nuclear import of the pathogenic polyglutamine-containing protein in cellular and animal models of polyglutamine diseases (Gatchel and Zoghbi, 2005).

Since human AR is widely expressed in various organs, nuclear accumulation of the pathogenic AR protein is detected not only in the central nervous system but also in nonneuronal tissues such as scrotal skin (Figs. 1D and E). The degree of pathogenic AR accumulation in scrotal skin epithelial cells tends to be correlated with that in the spinal motor neurons in autopsy specimens, and it is well correlated with CAG repeat length and inversely correlated with the motor functional scale (Banno et al., in press). These findings indicate that scrotal skin biopsy with anti-polyglutamine immunostaining is a potent biomarker with which to monitor SBMA pathogenic processes. Since SBMA is a slowly progressive disorder, appropriate biomarkers would help improve the power and cost effectiveness of longitudinal clinical treatment trials.

Molecular pathogenesis and therapeutic strategies

Ligand-dependent pathogenesis in animal models of SBMA

SBMA is unique among polyglutamine diseases in that the pathogenic protein, AR, has a specific ligand, testosterone, which alters the subcellular localization of the protein by favoring its nuclear uptake. AR is normally confined to a multiheteromeric inactive complex in the cell cytoplasm and translocates into the nucleus in a ligand-dependent manner. This ligand-dependent intracellular trafficking of AR appears to play important roles in the pathogenesis of SBMA.

In order to investigate ligand effect in SBMA, we generated transgenic mice expressing the full-length human AR containing 24 or 97 CAGs under the control of a cytomegalovirus enhancer and a chicken β-actin promoter (Katsuno et al., 2002). This model recapitulated not only the neurologic disorder but also the phenotypic difference with gender which is a specific feature of SBMA. The mice with 97CAGs (AR-97Q) exhibited progressive motor impairment, although those with 24 CAGs did not show any manifested phenotypes. Affected AR-97Q mice demonstrated small body size, short life span, progressive muscle atrophy, and weakness as well as reduced cage activity, all of which were markedly pronounced and accelerated in the male AR-97Q mice, but either not observed or far less severe in the female AR-97Q mice. The onset of motor impairment detected by the rotarod task was at 8 to 9 weeks of age in the male AR-97Q mice while 16 weeks or more in the females. The 50% mortality ranged from 66 to 132 days of age in the male AR-97Q mice, whereas mortality of the female AR-97Q mice remained only 10 to 30% at more than 210 days. Western blot analysis revealed the transgenic AR protein smearing from the top of the gel in the spinal cord, cerebrum, heart, muscle, and pancreas. Although the male AR-97Q mice had more smearing protein than their female counterparts, the female AR-97Q mice had more monomeric AR protein. The nuclear fraction contained the most of smearing pathogenic AR protein. Diffuse nuclear staining and less frequent NIs detected by 1C2, an antibody specifically recognizing the expanded polyglutamine tract, were demonstrated in the neurons of spinal cord, cerebrum, cerebellum, brainstem, and dorsal root ganglia as well as in nonneuronal tissues such as heart, muscle, and

pancreas. Male AR-97Q mice showed markedly more abundant diffuse nuclear staining and NIs than females, in agreement with the symptomatic and Western blot profile differences with gender. Despite the profound sexual difference of the pathogenic AR protein expression, there was no significant difference in the expression of the transgene mRNA between the male and female AR-97Q mice. These observations indicate that the testosterone level plays important roles in the sexual difference of phenotypes, especially in the post-transcriptional stage of the pathogenic AR.

The dramatic sexual difference of phenotypes led us to hormonal interventions in our mouse model. First, we castrated male AR-97Q mice in order to decrease their testosterone level. Castrated male AR-97Q mice showed profound improvement of symptoms, histopathologic findings, and nuclear localization of the pathogenic AR compared with the sham-operated male AR-97Q mice. Body weight, motor function, and lifespan of male AR-97Q mice were significantly improved by castration. Western blot analysis and histopathology revealed diminished nuclear accumulation of the pathogenic AR in the castrated male AR-97Q mice. Next, we administered testosterone to the female AR-97Q mice. In contrast to castration of the male mice, testosterone caused significant aggravation of symptoms, histopathologic features, and nuclear localization of the pathogenic AR in the female AR-97Q mice. Since the nuclear translocation of AR is ligand-dependent, testosterone appears to show toxic effects in the female AR-97Q mice by accelerating nuclear translocation of the pathogenic AR. On the contrary, castration prevented the nuclear localization of the pathogenic AR by reducing the testosterone level. The nuclear accumulation of the pathogenic AR protein with an expanded polyglutamine tract is likely essential in inducing neuronal cell dysfunction and degeneration in the majority of polyglutamine diseases. It thus appears logical that reduction in testosterone level improves phenotypic expression by preventing nuclear localization of the pathogenic AR. In support of this hypothesis, the ligand-dependent neurodegeneration has also been revealed in a fruit fly model of SBMA (Takeyama et al., 2002). Alternatively, castration may enhance protective effects of molecular chaperones, which are normally associated with AR and dissociate upon ligand binding.

Testosterone blockade therapy for SBMA

Successful treatment of AR-97Q mice with castration inspired us testosterone blockade therapies using leuprorelin and flutamide (Katsuno et al., 2003). Leuprorelin is a potent luteinizing hormone-releasing hormone (LHRH) analog suppressing the releases of gonadotrophins, luteinizing hormone and follicle-stimulating hormone. This drug has been used for a variety of sex hormone-dependent diseases including prostate cancer, endometriosis, and prepuberty. The primary pharmacological target of leuprorelin is the anterior pituitary. Through its agonizing effect on LHRH-releasing cells, it initially promotes the releases of gonadotrophins, resulting in transient increase in the serum level of testosterone or estrogens. After this surge, the continued use of this drug induces desensitization of the pituitary by reducing LHRH receptor binding sites and/or uncoupling of receptors from intracellular processes. Within about 2 to 4 weeks of leuprorelin administration, human serum testosterone level decreases to the extent achieved by surgical castration. The effects are maintained during the treatment, suggesting that continuous administration of leuprorelin is required for its clinical use. This drug thus has been provided as sustained release depot taking the form of polymer microspheres. On the other hand, flutamide, the first discovered androgen antagonist, has highly specific affinity for AR and competes with testosterone for binding to the receptor. It has been used for the treatment of prostate cancer, usually in association with an LHRH analog, in order to block the action of adrenal testosterone. Although flutamide suppresses the androgen-dependent transactivation, it does not reduce the plasma levels of testosterone.

Leuprorelin successfully inhibited nuclear accumulation of the pathogenic AR, resulting in marked amelioration of neuromuscular phenotypes seen in the male AR-97Q mice (Fig. 2). Leuprorelin initially increased the serum testosterone level by agonizing the LHRH receptor but subsequently reduced it to undetectable levels. Androgen blockade effects were also confirmed by reduced weights of the prostate and seminal vesicle. The leuprorelin-treated AR-97Q mice showed longer lifespan, larger body size, and better motor performance compared with vehicle-treated mice. Although leuprorelin-induced infertility was prevented by dose reduction, the therapeutic effects on neuromuscular phenotypes were insufficient at a lower dose of leuprorelin. In the Western blot analysis and anti-polyglutamine immunohistochemistry, the leuprorelin-treated male AR-97Q mice demonstrated a markedly diminished amount of the pathogenic AR in the nucleus, suggesting that leuprorelin successfully reduced nuclear AR accumulation. Testosterone, which was given from 13 weeks of age, markedly aggravated neurological symptoms and pathologic findings of leuprorelin-treated male AR-97Q mice. Leuprorelin appears to improve neuronal dysfunction by preventing ligand-dependent nuclear translocation of the pathogenic AR in the same way as castration. Given its minimal invasiveness and established safety, leuprorelin appears to be a promising therapeutic agent for SBMA. In a preliminary open trial, 6-month treatment with leuprorelin significantly diminished nuclear accumulation of pathogenic AR in the scrotal skin of patients, suggesting that androgen deprivation intervenes in the pathogenic process of human SBMA, as demonstrated in animal studies (Banno et al., in press). Another trial on a larger scale is currently underway to verify clinical benefits of leuprorelin for SBMA patients.

Leuprorelin-treated AR-97Q mice showed deterioration of body weight and rotarod task at the age of 8–9 weeks, when serum testosterone initially increased through the agonistic effect of leuprorelin. This change was transient and followed by sustained amelioration along with consequent suppression of testosterone production. The foot print analysis also revealed temporary exacerbation of motor impairment. Immunostaining of tail specimen, sampled from the same individual mouse, demonstrated an increase in the number of the muscle fibers with nuclear 1C2 staining at 4 weeks of leuprorelin administration,